Retrieval of spherical particle size distribution using ant colony optimization algorithm

Hong Qi (齐 宏), Biao Zhang (张 彪)*, Yatao Ren (任亚涛), Liming Ruan (阮立明), and Heping Tan (谈和平)

School of Energy Science and Engineering, Harbin Institute of Technology, Harbin 150001, China

**Corresponding author: zhb7772796@163.com*

Received August 1, 2013; accepted September 4, 2013; posted online November 4, 2013

The ant colony optimization (ACO) algorithm based on the probability density function is applied for the retrieval of spherical particle size distribution (PSD). The spectral extinction data based on the Mie theory and the Lambert–Beer Law served as input for estimating five commonly use monomodal PSDs, i.e., Rosin–Rammer distribution, normal distribution, logarithmic normal distribution, modified beta distribution, and Johnson's $S_{\rm B}$ distribution. The retrieval results show that the ACO algorithm has high feasibility and reliability, thus providing a new method for the retrieval of PSD.

OCIS codes: 290.2200, 120.5820, 300.6360.

doi: 10.3788/COL201311.112901.

Particle size has a direct effect on industrial processes, product quality, production security, and energy consumption. Thus, providing real-time measurements of particle size distribution (PSD) and particle concentration is highly required in online monitoring of granularity in the industry[1]. The retrieval of PSD with nonintrusive optical measurement has shown large potential[2]. Numerous light-scattering, particle-sizing techniques have been widely used, including total light scattering, angle light scattering, diffraction light scattering and dynamic light scattering[3]. The measurement range is from nanometers to millimeters. Among these techniques, light extinction measurement is probably the most advantageous because it does not need absolute calibration and can be used for *in situ* monitoring of micron or submicron particle systems with simple optical layout[4]. In spectral extinction particle sizing, the PSD can be obtained using the extinction data at multiple wavelengths. The data processing of this technique solves the Fredholm integral equation of the first kind, which is a classic ill-posed problem. In fact, inversion methods to obtain useful solutions to ill-posed problems are still active research areas[5].

Generally, inversion methods can be divided into two different categories: independent mode and dependent mode. The independent mode does not need any assumptions on the PSD in advance. The PSD is retrieved by solving the discrete linear equation set. In the dependent mode, certain assumptions have to be made on the function form of the PSD beforehand, and the PSD is retrieved through some optimization algorithms[6]. Many random search intelligent algorithms have been successfully employed to retrieve PSD problems, such as artificial neural networks[7], particle swarm optimization[2], and genetic algorithms[8]. The ant colony optimization (ACO) algorithm is a potential heuristic bionic evolutionary algorithm first proposed in 1 991 by Colorni *et al*[9] based on the observation of the foraging behavior of real ants. Since 1 996, the ACO algorithm has drawn much attention worldwide, and its applications have expanded rapidly to many fields. Numerous studies show that ACO algorithm has positive feedback, parallelism, and robustness[10].

However, to the best of our knowledge, few reports have discussed the application of ACO algorithm to PSD problems. In this letter, we attempt to apply the ACO algorithm in the retrieval of spherical PSD based on probability density function (PDF). Firstly, three commonly used monomodal PSDs, namely, Rosin–Rammer (R-R) function, normal (N-N) function, and logarithmic normal (L-N) function, are retrieved in the dependent mode. Two proper versatile functions, namely, modified beta (M-β) function and Johnson's $S_{\rm B}$ (J-$S_{\rm B}$) function, are used to retrieve the above three commonly used monomodal PSDs.

The fundamental principle of retrieval based on the spectral extinction technique is the Lambert–Beer Law. When a parallel monochromatic light beam of intensity I_0 travels through a suspension of particle system, scattering and absorption lead to the attenuation of the transmitted light. When multiple scattering and interaction processes are neglected, the transmitted light intensity I with the incident wavelength λ can be calculated as[11]

$$\ln\left(\frac{I}{I_0}\right)_\lambda = -\frac{3}{2}\times L\times N\times\int_{D_{\min}}^{D_{\max}}\frac{Q_{\rm ext}(\lambda,\, m,\, D)}{D}f(D){\rm d}D, \tag{1}$$

where $(I/I_0)_\lambda$ is the extinction value of the monochromatic light at λ, which is a known parameter in the retrieval process and can be obtained through experimental measurement. L is the optical path length; N is the total number of particles; $D_{\min}$ and $D_{\max}$ are the lower and upper integration limits, respectively; $Q_{\rm ext}(\lambda,\, m,\, D)$ is the extinction efficiency of a single spherical particle, which is a function of the particle diameter D; λ is the wavelength; m is the relative refractive index that can be calculated by using the exact Mie theory or estimated by using appropriate approximation methods. $f(D)$ is the volume frequency distribution function, and also the PSD function that we want to determine.

As social insects, ants live in colonies and their behav-

iors are governed by the goal of colony survival rather than the survival of individuals. In the process of looking for food, ants leave chemical pheromones, an evaporable material, on the ground so that other ants can smell it. The concentration of the pheromone depends on the quality and quantity of the food source. Ants tend to choose paths with high pheromone concentrations. The original ACO algorithm is introduced to solve discrete domain optimization problems. However, the retrieval of spherical PDF is a continuous domain optimization problem. Several types of ACO algorithms can be used for continuous domain optimization problems. The PDF-based ACO algorithm is one of the most efficient. The logical adaption would be to shift from the discrete probability distribution to a continuous PDF[12].

The number of inversion parameters is set as $N_{\rm p}$, the total number of the ants is set as $N_{\rm m}$, and the amount of the dominant ant ranks is set as $N_{\rm n}$. The search space $[{\rm low_i}, {\rm high_i}]$ of each inversion parameter needs to be estimated before the optimization process. In each of the $N_{\rm p}$ construction steps, an ant chooses a value $x_{\rm i}$ for exactly one of the dimensions. To make this choice, an ant uses a Gaussian kernel, which is a weighted superposition of several Gaussian functions, as the PDF. The probability density distribution of the ith inversion parameter of the jth rank at iteration t is expressed as

$$P_{i,\,j}(t) = w_j \cdot f_{i,\,j}(t), \tag{2}$$

where w_j denotes the probability of selecting the jth rank determined by the pheromone value τ_j and $f_{i,\,j}(t)$ is the probability density distribution which is a normal distribution with expectation $\mu_{i,\,j}(t)$ and standard deviation $\sigma_{i,\,j}(t)$.

The probability of selecting the jth rank w_j is defined as

$$w_j = \tau_j \Big/ \sum_{m=1}^{N_{\rm n}} \tau_m, \tag{3}$$

where τ_j denotes the pheromone value of the jth rank, and is defined as

$$\tau_j = \frac{1}{\alpha N_{\rm n}\sqrt{2\pi}} \exp\left[-\frac{(j-1)^2}{2\alpha^2 N_{\rm n}^2}\right], \tag{4}$$

where α is a positive parameter that determines the relative weight of the rank.

The probability density distribution of a normal distribution $f_{i,\,j}(t)$ is defined as[13]

$$f_{i,\,j}(t+1) = \frac{1}{\sqrt{2\pi}\sigma_{i,\,j}(t)} \exp\left\{-\frac{[x_i - \mu_{i,\,j}(t)]^2}{2\sigma_{i,\,j}^2(t)}\right\}, \tag{5}$$

where $\mu_{i,\,j}(t)$ is the retrieval value of the ith inversion parameter with the jth rank at iteration t. $\sigma_{i,\,j}(t)$ is the standard deviation of the ith inversion parameter with the jth rank at iteration t, and can be defined as

$$\sigma_{i,\,j}(t) = \beta \sqrt{\frac{1}{N_{\rm n}} \sum_{l=1}^{N_{\rm n}} \Big[\mu_{i,\,l}(t) - \mu_{i,\,j}(t)\Big]^2}, \tag{6}$$

where β is a positive parameter that regulates the speed of convergence. A higher value of β corresponds to a lower convergence speed of the algorithm.

After the ant selects the value $x_{\rm i}$ for all of the inversion parameters, the estimated values can be calculated by the direct model. Furthermore, the value of the objective function, which relates the estimated values to the measured values, can be obtained. When all the ants select the values, one iteration cycle completes. The dominant ants, which have the smallest N_n values of the objective function, are generated. Smaller values of the objective function correspond to a higher rank. The expectation $\mu_{i,\,j}(t)$ and the standard deviation $\sigma_{i,\,j}(t)$ of the PDF must be updated. The next iteration cycle does not start unless the program matches one of the following three-stop criteria:

(a) The value of the objective function is less than the tolerance ε, $F_{\rm obj} < \varepsilon$;

(b) The largest standard deviation is less than the setting value ξ, $\max\{\sigma_{i,\,j}(t)\} < \xi$;

(c) The number of the iteration reaches the user-defined iteration limit $N_{\rm c}$, ${\rm iter}(t) < N_{\rm c}$.

Many particle systems conform to two-parameter size distributions, so the PSD is easier to retrieve in dependent mode, where the most widely used distribution functions are the R-R, N-N, and L-N functions. The mathematical representations of their monomodal volume frequency distributions are[2]

$$f_{\rm R-R}(D) = \frac{k}{\bar{D}} \times \left(\frac{D}{\bar{D}}\right)^{k-1} \times \exp\left[-\left(\frac{D}{\bar{D}}\right)^k\right], \tag{7}$$

$$f_{\rm N-N}(D) = \frac{1}{\sqrt{2\pi}\sigma_{\rm N}} \times \exp\left[-\frac{(D-\mu_{\rm N})^2}{2\sigma_{\rm N}^2}\right], \tag{8}$$

$$f_{\rm L-N}(D) = \frac{1}{\sqrt{2\pi}D\ln\sigma_{\rm L}} \times \exp\left[-\frac{(\ln D - \ln\mu_{\rm L})^2}{2\,(\ln\sigma_{\rm L}^2)^2}\right], \tag{9}$$

where $\bar{D}$, k, $\mu_{\rm N}$, $\sigma_{\rm N}$, $\mu_{\rm L}$, and $\sigma_{\rm L}$ are the characteristic parameters. The complex refraction index used in this letter refers to practical situations. For instance, the real part n and imaginary part k of the coal ash particle's typical complex refractive index are in the ranges of $n \in [1.18,\ 1.92]$ and $k \in [0.01,\ 1.13]$[14], respectively. The complex refractive index is selected as $1.51 + 0.03i$, which is assumed to be independent of the wavelength for the sake of simplicity.

The incident beam is set as two wavelengths $\lambda = 0.4$, 0.8 μm or five wavelengths $\lambda = 0.4$, 0.5, 0.6, 0.7, and 0.8 μm. The overall particle size measurement range is limited from 0.1 to 10 μm in diameter, which is the optimal measurement range in the spectral extinction particle size technique. The true values of this distribution are set as $(\bar{D},\, k) = (3.0,\, 7.55)$, $(\mu_{\rm N},\, \sigma_{\rm N}) = (3.6,\, 2.4)$, and $(\mu_{\rm L},\, \sigma_{\rm L}) = (3.0,\, 1.2)$. The PDF-based ACO algorithm is used to retrieve these three spherical PSDs in the dependent mode, and the system control parameters of the ACO algorithm are shown in Table 1.

The retrieval of spherical PSDs is solved through the minimization of the objective function, which is the sum of the square residuals between the estimated and mea-

sured transmittance ratios as

$$F_{\text{obj}} = \sum_{i=1}^{N_\lambda} \left\{ \frac{[(I/I_0)_\lambda]_{\text{est}} - [(I/I_0)_\lambda]_{\text{mea}}}{[(I/I_0)_\lambda]_{\text{mea}}} \right\}^2. \quad (10)$$

Considering that the ACO algorithm is a stochastic optimization method, and all optimizations have certain randomness, the ACO algorithm is repeated 100 times for each of the three PSDs. The retrieval results are shown in Figs. 1–3 and Table 2.

As shown in Table 2, the accuracy of the PDF-based ACO algorithm is very high, even with a measurement noise of 10%. The mean relative error and the standard deviation of the inversion parameters increase when the measurement noise increases. We can infer that the ACO algorithm has high feasibility and reliability in the retrieval of the PSD problems. Figures 1–3 indicate that the retrieval result of five wavelengths is better than that of two wavelengths. The reason may be that two wavelengths supply less transmitted light information, leading to easier acquisition of multivalued retrieval results compared with using five wavelengths.

However, for many particle circumstances, the forms of the distributions are usually unknown beforehand. Generally, no single distribution function can represent all

Table 1. Parameters of the PDF-based ACO Algorithm for Different PSD Functions

Parameter	Value
N_p	2
N_m	30
N_n	5
N_c	1 000
[low, high]	[0, 150]
α	0.5
β	0.7
ε	10^{-6}
ξ	10^{-6}

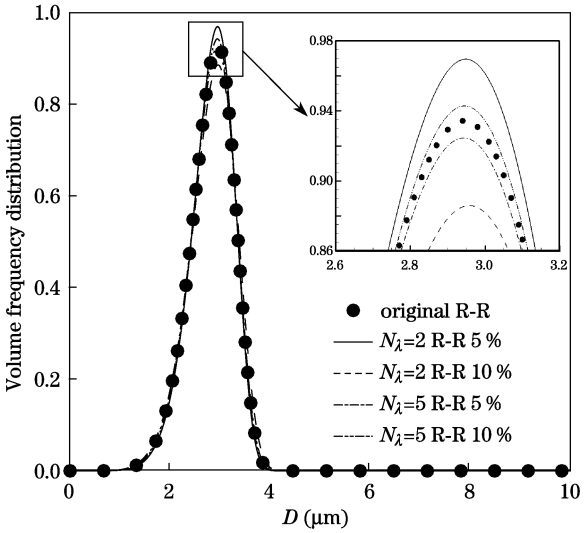

Fig. 1. Retrieval results of the R-R function with $(\bar{D}, k) = (3.0, 7.55)$ using two or five wavelengths under measurement noise.

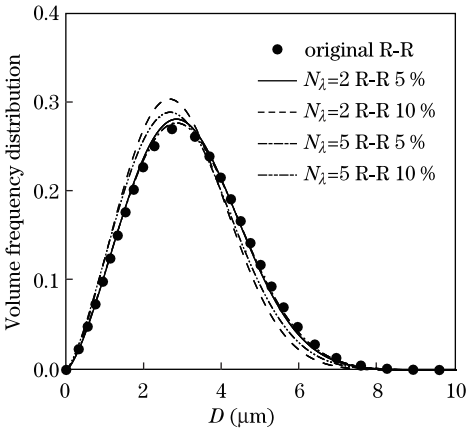

Fig. 2. Retrieval results of the N-N function with $(\mu_N, \sigma_N) = (3.6, 2.4)$ using two or five wavelengths under measurement noise.

Table 2. Retrieval Results of the Three PSD Functions with Two or Five Wavelengths

Function		Two Wavelengths		Five Wavelengths	
	Noise	$\bar{D}$	k	$\bar{D}$	k
R-R $(\bar{D}, k) = (3.0, 7.55)$	0%	$3.00\pm7.52\times10^{-7}$	$7.55\pm3.68\times10^{-5}$	$3.00\pm4.37\times10^{-7}$	$7.55\pm3.68\times10^{-6}$
	5%	$3.00\pm4.01\times10^{-2}$	$7.84\pm1.57\times10^{0}$	$3.00\pm2.50\times10^{-2}$	$7.47\pm4.67\times10^{-1}$
	10%	$3.02\pm8.01\times10^{-2}$	$7.20\pm2.00\times10^{0}$	$3.00\pm4.79\times10^{-2}$	$7.62\pm9.27\times10^{-1}$
	Noise	μ_N	σ_N	μ_N	σ_N
N-N $(\mu_N, \sigma_N) = (3.6, 2.4)$	0%	$3.60\pm1.18\times10^{-6}$	$2.40\pm3.78\times10^{-6}$	$3.60\pm5.86\times10^{-7}$	$2.40\pm1.83\times10^{-6}$
	5%	$3.52\pm1.48\times10^{-1}$	$2.44\pm3.19\times10^{-1}$	$3.54\pm1.32\times10^{-1}$	$2.41\pm2.89\times10^{-1}$
	10%	$3.28\pm5.40\times10^{-1}$	$2.46\pm5.41\times10^{-1}$	$3.36\pm4.32\times10^{-1}$	$2.38\pm5.34\times10^{-1}$
	Noise	μ_L	σ_L	μ_L	σ_L
L-N $(\mu_L, \sigma_L) = (3.0, 1.2)$	0%	$3.00\pm3.07\times10^{-4}$	$1.20\pm1.78\times10^{-2}$	$3.00\pm2.81\times10^{-6}$	$1.20\pm3.11\times10^{-6}$
	5%	$3.01\pm3.44\times10^{-2}$	$1.22\pm9.12\times10^{-2}$	$3.00\pm2.92\times10^{-2}$	$1.20\pm2.73\times10^{-2}$
	10%	$3.01\pm6.25\times10^{-2}$	$1.24\pm1.37\times10^{-1}$	$3.01\pm5.03\times10^{-2}$	$1.21\pm5.10\times10^{-2}$

*The mean and standard deviation of the 100-time retrieval results are shown as $a \pm b$ in the table.

PSDs encountered in reality, but several versatile functions exist that can represent most of the commonly used PSDs. Popplewell and Yu suggested that the M-β function and the J-$S_{\rm B}$ function, respectively, can be used as general functions to represent the monomodal PSDs. The functions are described as[15]

$$f_{{\rm M}-\beta}(D)=\frac{(D-D_{\min})^{\alpha m}(D_{\max}-D)^{m}}{\int_{D_{\min}}^{D_{\max}}(D-D_{\min})^{\alpha m}(D_{\max}-D)^{m}{\rm d}D}. \quad (11)$$

$$f_{{\rm S_B}}(D)=\frac{\sigma_{\rm S}}{\sqrt{2\pi}}\times\frac{D_{\max}-D_{\min}}{(D-D_{\min})(D_{\max}-D)}\times\exp$$

$$\left\{-\frac{\sigma_{\rm S}^2}{2}\left[\ln\left(\frac{D-D_{\min}}{D_{\max}-D}\right)-\ln\left(\frac{M-D_{\min}}{D_{\max}-M}\right)\right]^2\right\}, \quad (12)$$

where α, m, $\sigma_{\rm S}$, and M are the characteristic parameters.

The M-β function and the J-$S_{\rm B}$ function are used to retrieve the monomodal R-R, N-N, and L-N PSDs with five wavelengths. The system control parameters of the PDF-based ACO algorithm are set to be the same as those in Table 1. The reproducibility of the PDF-based ACO algorithm for the original R-R distribution is given in Table 3 and Fig. 4 with $(\bar{D},\, k) = (2.0,\, 7.0)$. Meanwhile, the reproducibility of the original N-N distribution is given in Table 4 and Fig. 5 with $(\mu_{\rm N},\, \sigma_{\rm N}) = (5.0,\, 1.2)$, and the original L-N distribution with $(\mu_{\rm L},\, \sigma_{\rm L}) = (6.0,\, 1.15)$ in Table 5 and Fig. 6. To investigate the reliability of this method, the inversion error $\varepsilon_{\rm ret}$ is used to characterize the quality of the retrieval results

$$\varepsilon_{\rm ret}=\left\{\frac{\sum_{i=1}^{100}\left[f_{\rm ret}(\widetilde{D}_i)-f_{\rm ori}(\widetilde{D}_i)\right]^2}{\sum_{i=1}^{100}\left[f_{\rm ori}(\widetilde{D}_i)\right]^2}\right\}^{1/2}, \quad (13)$$

where $\widetilde{D}_i$ is the midpoint of the ith subinterval $[\widetilde{D}_i,\, \widetilde{D}_{i+1}]$ of the particle size range $[D_{\min}, D_{\max}]$; $f_{\rm ori}(\widetilde{D}_i)$ and $f_{\rm ret}(\widetilde{D}_i)$ are the original and retrieval volume frequency distribution, respectively, in the ith subinterval.

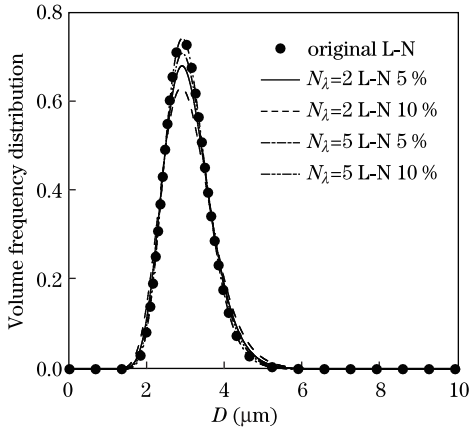

Fig. 3. Retrieval results of the L-N function with $(\mu_{\rm L},\, \sigma_{\rm L}) = (3.0,\, 1.2)$ using two or five wavelengths under measurement noise.

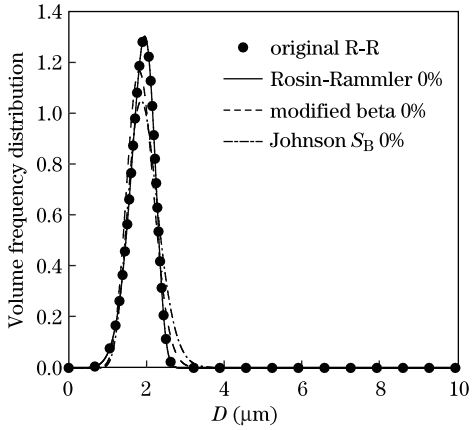

Fig. 4. Reproducibility of the R-R function with $(\bar{D},\, k) = (2.0,\, 7.0)$ by the M-β function and the J-$S_{\rm B}$ function under absence of noise.

Table 3. Reproducibility of R-R with $(\bar{D}, k) = (2.0, 7.0)$ by the Two General Functions

Function Parameter		Noise 0%		Noise 2%		Noise 5%	
		Results	$\varepsilon_{\rm ret}$	Results	$\varepsilon_{\rm ret}$	Results	$\varepsilon_{\rm ret}$
$f_{\rm R-R}$	$\bar{D}$	2.00000	0.00000	2.00051	0.00121	2.00251	0.00677
	k	7.00000		7.00169		7.03319	
$f_{{\rm M}-\beta}$	α	0.20959	0.20538	0.20955	0.20539	0.21078	0.19719
	m	98.12641		98.50675		96.41465	
$f_{{\rm J}-S_{\rm B}}$	$\sigma_{\rm S}$	3.86498	0.22220	3.97606	0.20750	3.95521	0.20819
	M	1.92910		1.89676		1.90337	

Table 4. Reproducibility of R-R with $(\mu_{\rm N}, \sigma_{\rm N}) = (5.0, 1.2)$ by the Two General Functions

Function Parameter		Noise 0%		Noise 2%		Noise 5%	
		Results	$\varepsilon_{\rm ret}$	Results	$\varepsilon_{\rm ret}$	Results	$\varepsilon_{\rm ret}$
$f_{\rm N-N}$	$\mu_{\rm N}$	5.00000	0.00000	5.00442	0.00027	5.03173	0.00261
	$\sigma_{\rm N}$	1.20000		1.20110		1.22616	
$f_{{\rm M}-\beta}$	α	1.15562	0.22255	1.20379	0.27268	1.30244	0.37392
	m	6.59748		6.20693		6.14235	
$f_{{\rm J}-S_{\rm B}}$	$\sigma_{\rm S}$	2.02292	0.00365	2.03383	0.00365	1.97946	0.04213
	M	4.96741		4.96520		5.02525	

Table 5. Reproducibility of L-N with $(\mu_{\rm L}, \sigma_{\rm L}) = (6.0, 1.15)$ by the Two General Functions

Function	Parameter	Noise 0%		Noise 2%		Noise 5%	
		Results	$\varepsilon_{\rm ret}$	Results	$\varepsilon_{\rm ret}$	Results	$\varepsilon_{\rm ret}$
$f_{\rm L-N}$	$\mu_{\rm L}$	6.00000	0.00000	6.01081	0.00429	6.18539	0.16216
	$\sigma_{\rm L}$	1.15000		1.15820		1.16809	
$f_{\rm M-\beta}$	α	1.69380	0.26166	1.84769	0.38978	1.71335	0.27884
	m	9.34964		8.53924		8.89997	
$f_{\rm J-S_B}$	$\sigma_{\rm S}$	2.71091	0.13465	2.73354	0.13336	2.67170	0.16451
	M	6.06498		6.06533		6.11148	

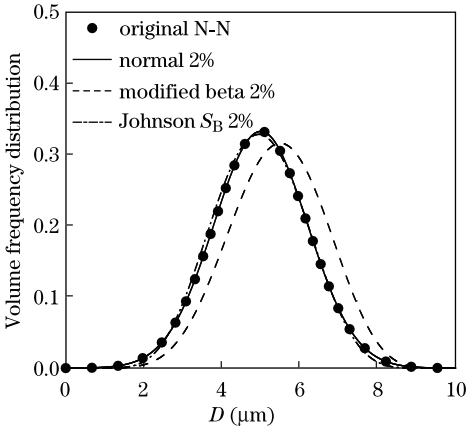

Fig. 5. Reproducibility of the N-N function with $(\mu_{\rm N}, \sigma_{\rm N}) = (5.0, 1.2)$ by the M-β function and the J-$S_{\rm B}$ function under 2% noise.

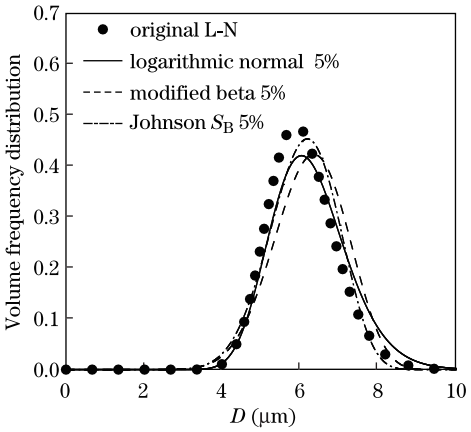

Fig. 6. Reproducibility of the L-N function with $(\mu_{\rm L}, \sigma_{\rm L}) = (6.0, 1.15)$ by the M-β function and the J-$S_{\rm B}$ function under 5% noise.

As can be seen from Tables 3–5 and Figs. 4–6, a reasonable agreement exists between the two general functions and the original functions. If no noise is added to the extinction data, the reproducibility by the original function is much better than that of the general functions. The reproducibility by the original function deteriorates sharply with the increase of the measurement noise. The reproducibilities by the two general functions are relatively more stable than those of the original function within 5% noise.

In conclusion, the PDF-based ACO algorithm is firstly applied to the retrieval of spherical PSD, thereby providing a new method. By retrieving the PSD in the dependent mode, the inversed parameters can be estimated accurately even with noisy data by the ACO algorithm. This algorithm is demonstrated to have high feasibility and reliability, establishing its potential to be implemented to solve various PSD problems. The existence of such a general PSD function is validated through the reproducibility of the most widely used monomodal PSDs, in which the M-β function and the J-$S_{\rm B}$ function are used as the assumed types of the PSDs. Our future directions are twofold. On one hand, we would like to look for other general functions; on the other hand, we want to further improve the performance of the ACO methodology, so that we can apply it to other bimodal, multimodal, and mixed PSD problems in independent mode.

This work was supported by the Foundation for Innovative Research Groups of the National Natural Science Foundation of China (No. 51121004), the National Natural Science Foundation of China (No. 51076037), and the Fundamental Research Funds for the Central Universities (No. HIT. BRET 1. 2010012). A very special acknowledgement is made to the editors and referees who made important comments to improve this letter.

References

1. C. Feng, L. Huang, J. Wang, Y. Zhao, and H. Huang, Chin. Opt. Lett. **9,** 092901 (2011).
2. H. Qi, L. Ruan, S. Wang, M. Shi, and H. Zhao, Chin. Opt. Lett. **6,** 346 (2008).
3. W. Cai and L. Ma, Chin. Opt. Lett. **10,** 012901 (2012).
4. H. Tang, X. Sun, and G. Yuan, Chin. Opt. Lett. **5,** 31 (2007).
5. L. Wang, X. Sun, and J. Xing, J. Modern Opt. **59,** 1829 (2012).
6. H. Tang and J. Lin, J. Quantitative Spectroscopy and Radiative Transfer **115,** 78 (2013).
7. R. Guardani, C. A. O. Nascimento, and R. S. Onimaru, Powder Technology **126,** 42 (2002).
8. H. Tang and G. Liang, Powder Technology **198,** 330 (2010).
9. A. Colorni, M. Dorigo, and V. Maniezzo, in *Proceedings of the first European conference on artificial life* 134 (1991).
10. M. Dorigo and T. Stützle, *Ant Colony Optimization* (Massachusetts Institute of Technology Press, Cambridge, 2004).
11. L. Wang, X. Sun, and F. Li, Appl. Opt. **51,** 2997 (2012).
12. C. Blum, Phys. Life Rev. **2,** 353 (2005).
13. K. Socha, in *Proceedings of the 4th International Workshop on Ant Colony Optimization and Swarm Intelligence* 25 (2004).
14. L. Ruan, Q. Yu, and H. Tan, J. Harbin Institute of Technology, **1,** 10 (1994).
15. H. Tang, Thermal Science **16,** 1400 (2012).